Comparison of the cloud top heights retrieved from MODIS and AHI satellite data with ground-based Ka-band radar

Juan Huo, Daren Lu, Shu Duan, Yongheng Bi, Bo Liu

Key Laboratory for Atmosphere and Global Environment Observation, Chinese Academy of Sciences, Bejing, 100029, China

5 *Correspondence to:* Juan Huo (huojuan@mail.iap.ac.cn)

Abstract. To better understand the accuracy of cloud top heights (CTHs) derived from passive satellite data, ground-based Ka-band radar measurements from 2016 and 2017 in Beijing were compared with CTH data inferred from the Moderate Resolution Imaging Spectroradiometer (MODIS) and the Advanced Himawari Imager (AHI). Relative to the radar CTHs, the MODIS CTHs were found to be underestimated by −1.10 ± 2.53 km and 49% of CTH differences were within 1.0 km. Like the

10 MODIS results, the AHI CTHs were underestimated by −1.10 ± 2.27 km and 42% were within 1.0 km. Both the MODIS and AHI retrieval accuracy depended strongly on the cloud depth (CD). Large differences were mainly occurring for the retrieval of thin clouds of CD < 1 km, especially clouds higher than 4 km. For clouds with CD > 1 km, the CTH difference decreased to −0.48 ± 1.70 km for MODIS and to −0.76 ± 1.63 km for AHI. MODIS CTHs greater than 6 km showed better agreement with the radar data than those less than 4 km. Statistical analysis showed that the average AHI CTHs were lower than the average

15 MODIS CTHs by −0.64 ± 2.36 km. The monthly accuracy of both retrieval algorithms was studied and it was found that the AHI retrieval algorithm had the largest bias in winter while the MODIS retrieval algorithm had the lowest accuracy in spring.

1 Introduction

Clouds have a great impact on the water and energy budgets in the Earth–atmosphere system (Ramanathan et al. 1989; Liou 1992; Cess et al. 1996; Boucher et al. 2013). Clouds are one of the least-understood components and constitute one of the

20 largest sources of uncertainty in general circulation model (GCM) simulations as cloud vertical distributions determine the diabatic heating profiles (Wetherald and Manabe 1988; Arakawa 2004). Cloud top height (CTH) is one of the important cloud

parameters that provide information on the vertical structure of cloud water content (Stubenrauch et al. 1997;Marchand et al. 2010). Comparisons of modeled stratocumulus CTHs with satellite retrievals suggest that either satellite retrievals place stratocumulus clouds too high in the atmosphere or GCMs cloud tops are biased low (Rossow and Schiffer 1999). Knowledge

25 of CTH is crucial to understand the Earth's radiation budget and global climate change.

Active and passive instruments have long been used for monitoring CTHs (Atlas 1954; Schiffer and Rossow 1983; Pavolonis and Heidinger 2004; Stephens and Kummerow 2007; Huo and Lu 2009; Görsdorf et al. 2015). Active instruments, i.e., cloud radars and lidars, detect CTH directly through reflectivity from cloud top particles. Passive infra-red (IR) instruments measure the IR brightness temperature of cloud to derive CTH based on assumptions, for instance, cloud is

30 regarded as a black body. Surface measurements and satellite measurements have different strengths and weaknesses. Surface active instruments are ideal sensors for accurately detecting the CTH. Yet, surface instruments are limited in spatial scale. Satellites measure large-scale cloud systems, but the CTHs retrieved from passive IR instruments are still subject to large uncertainties. This study assesses the accuracy of the CTHs derived from passive satellites through comparison with surface active radar data.

35 The Moderate Resolution Imaging Spectroradiometer (MODIS) onboard the Aqua and Terra satellites has been in service since 2000 and the cloud products are being widely used by the meteorological community (King et al. 1998; Ackerman 1998; Rodell and Houser 2004; Roskovensky and Liou 2006; Remer et al., 2008; Pincus et al., 2012). Uncertainties in the MODIS CTH products have been assessed using many measurements, i.e., from the ground, aircraft and satellites (Naud et al. 2002; Weisz et al. 2007; Ham et al. 2009; Chang et al. 2010; Marchand et al. 2010; Baum et al. 2012; Marchand 2013; Xi et al. 2014).

40 Frey et al. (1999) reported that the retrieved CTHs from the MODIS airborne simulator were within ±1.5 km of the CTHs from the Cloud Lidar System. Naud and Muller (2002) showed that the two sets of averaged CTHs from the Multi-Angle Imaging Spectroradiometer (MISR) and MODIS were generally within 2 km of each other over the British Isles. Holz et al. (2008) found that MODIS underestimated the CTH relative to the Cloud-Aerosol Lidar with Orthogonal Polarization (CALIOP) by 1.4 ± 2.9 km globally over a two-month period. Clouds have strong regional characteristics. Evaluation results from previous

45 studies are not representative of specific regions. This study compares the retrieved MODIS CTHs with radar measurements in Beijing over a long period.

The Advanced Himawari Imager (AHI) onboard the Himawari-8 (HW8) satellite, a geostationary meteorological satellite, has provided CTHs since July 2015 (Bessho et al. 2016). Zhou et al. (2019) reported that the CTHs derived from surface Ka-band radar, from December 2016 to November 2017, are 0.82 km higher than those retrieved from the AHI radiance data

50   based on a Fengyun Geostationary Algorithm Testbed-Imager (FYGAT-I) science product algorithm (Min et al. 2017). Mouri et al. (2016) found that the CTH was underestimated compared with the MODIS and CALIOP data over two weeks of measurements. The AHI CTH retrievals are, relatively, new to the meteorological community and require further evaluation before application in meteorological studies.

MODIS and AHI share some common retrieval principles and technologies for CTH. However, their retrieval

55   algorithms are different in terms of the radiative transfer model, atmospheric profiles, source measurements and cloud types. A Ka-band (35.075 GHz) radar at the Institute of Atmospheric Physics in Beijing, China (39.96°N, 116.37°E) has been used for cloud measurements since 2012 (Huo et al. 2019). In this study, we compare and evaluate the CTHs retrieved from the passive satellite instruments onboard a polar-orbiting satellite and a geostationary satellite with those measured by a surface active radar in Beijing over a long period. To our knowledge, this study presents the first comparison and evaluation of the

60   CTH datasets for Beijing from MODIS and AHI. This work quantifies the satellite CTH retrieval accuracy and provides a reference and usage guidance for the application of the CTH datasets in meteorological research, such as climate models for Beijing and North China.

2. Description of the MODIS, AHI and Ka-band radar CTH retrievals

2.1 MODIS CTH retrieval

65   MODIS measures radiance in 36 spectral bands from 0.42 to 14.24 μm at three spatial resolutions: 250 m, 500 m and 1000 m. The swath dimensions are 2330 km (cross-track) by 10 km (along-track at nadir). MODIS cloud top pressure (height) is determined by a combination algorithm of CO_2-slicing technology (also known as the radiance ratioing technology) and infrared-window technology (IRW, using the 11 μm brightness temperature, Smith and Platt 1978; Nieman et al. 1993) in conjunction with the National Centers for Environmental Prediction Global Data Assimilation System temperature profiles

70 (Menzel 2008; Baum et al. 2012). Equations (1)–(3) present the theory of the CO_2-slicing technology. The CO_2-slicing

technique is used to determine CTHs for mid- or upper-level clouds, and the CTHs of low-level clouds are inversed by the IRW.

When the radiance difference between cloud and clear sky is so small at 15 μm that CO_2-slicing technology is unsuitable for

CTH retrieval, the IRW is applied.

$$R(v) = (1 - NE)\,R_{clr}(v) + NE\,[R_{bcd}(v, P_c)], \quad (1)$$

$$R_{bcd}(v,P_c) = R_{clr}(v) - \int_{P_c}^{P_s} \tau(v,p)\,\frac{\mathrm{d}B[v,T(p)]}{\mathrm{d}p}, \quad (2)$$

$$\frac{R(v_1)-R_{clr}(v_1)}{R(v_2)-R_{clr}(v_2)} = \frac{NE_1 \int_{P_s}^{P_c} \tau(v_1,p)\,\frac{\mathrm{d}B[v_1,T(p)]}{\mathrm{d}p}}{NE_2 \int_{P_s}^{P_c} \tau(v_2,p)\,\frac{\mathrm{d}B[v_2,T(p)]}{\mathrm{d}p}}, (3)$$

where v is the frequency, E is the emissivity of cloud, $R(v)$ is the radiance measured, R_{clr} is the radiance of clear sky, N is the

75 cloud coverage of the field of view in the range of 0~1, $\tau(v, p)$ is the fractional transmittance of radiation at the wavelength v

from the atmospheric pressure level (p) arriving at the top of the atmosphere ($p = 0$), P_c is the cloud top pressure, $B[v, T(p)]$

is the Planck radiance at the wavelength v at the temperature $T(p)$, and P_s is the surface pressure.

   Terra-MODIS CTHs are retrieved based on the channels 36/35 and 35/33 (corresponding to 14.2/13.94 μm and

13.94/13.34 μm) ratio pairs due to noise problems at band 34; Aqua-MODIS CTHs are retrieved by the three ratio pairs:

80 channels 36/35, channels 35/34, channels 34/33 (14.2/13.94 μm, 13.94/13.64 μm, 13.64/13.34 μm). Most published

evaluation studies on the MODIS cloud top properties are from the Collection-5 version datasets. Compared with the

Collection-5 version algorithm, Collection-6 differs in terms of the radiative transfer model calculation, for example, using

ozone profiles provided in the meteorological products rather than from climatological values, the spatial resolution and

application of the CO_2-slicing method to only ice clouds (Baum et al. 2012). The MODIS cloud products used in this study

85 are the Collection-6 version cloud datasets (MYD06/MOD06) from both Aqua and Terra at 1 km spatial resolution.

2.2 AHI CTH retrieval

The HW8 satellite, equipped with the AHI, was launched on 7 October 2014 at the location of 140.7°E and its operation by

the Japanese Meteorological Agency commenced on 7 July 2015 (Bessho et al. 2016). The AHI is a visible infrared

radiometer that has 16 observation bands, ranging from 0.47 to 13.3 μm (3 for visible, 3 for near-infrared and 10 for infrared).

90   The AHI observes the Japanese and some other target or landmark areas every 2.5 min and the entire full disk every 10 min

with a spatial resolution of 0.5–2.0 km. The scan ranges for full disk and the Japanese area are preliminarily fixed, while

those for the target area and landmark areas are flexible to meteorological conditions. Relative to the imagers onboard

previous Japanese geostationary satellites, the AHI is improved in terms of the number of bands, spatial resolution, temporal

frequency and radiometric calibration.

95   The AHI CTH retrieval algorithm involves the use of radiative transfer codes (Eyre 1991) developed by EUMETSAT,

input with Numerical Weather Prediction temperature and humidity profile data, to calculate the radiance of four infrared

bands (wavelengths 6.2, 7.3, 11.2 and 13.3 μm). The CTH is determined by the interpolation method (for opaque and

fractional cloud, similar to the IRW), the intercept method (for semi-transparent cloud) and the CO_2-slicing method (Neiman

et al 1993, Schmetz et al. 1993, Mouri et al. 2016). In the retrieval process for optically thin (or semi-transparent) clouds, if

100   the intercept method does not produce suitable results, the CO_2-slicing method is applied; if this also fails to produce

suitable results, the interpolation method is utilized. The AHI cloud products used in this study are the Himawari-8 Cloud

Property data released through the JAXA's P-Tree System (https://www.eorc.jaxa.jp/ptree/index.html).

2.3 Ka-band radar

The Ka-band polarization Doppler radar (Ka radar, wavelength 8.55 mm), situated at the Institute of Atmospheric Physics

105   (IAP, 39.967°N, 116.367°E), was set up in 2010 (Fig. 1). The technical specifications of the Ka-band radar are given in

Table 1. The Ka radar works 24 h a day in a vertically pointing mode, except during special events, such as heavy rain or

short-term collaborative observations with other instruments, when the mode is changed.

Fig. 1. The Ka-band polarization Doppler radar at the Institute of Atmospheric Physics, Chinese Academy of Physics,

110   Beijing, China (39.967°N, 116.367°E).

A data quality control approach using a combination of the threshold and median filter methods has been implemented to

reduce the effects of clutter and noise on the radar reflectivity (Xiao et al. 2018). It is considered to be cloudy if the

reflectivity profile contains more than three bins of radar reflectivity data higher than −45 dBZ. Zhou et al. (2019) used a

115   threshold of −40 dBZ for cloud determination for their Ka radar, the transmitter of which was a different type compared with

the IAP radar. A lower threshold might neglect some clouds with weak returns.

120

Table 1. Main technical specifications of the Ka-band radar at the IAP.

Parameters		Technical Specification
Transmitter	Frequency	35.075GHz
	Peak power	29kW
	Pulse length	0.2μs
	Type	Magnetron
Antenna	Diameter	1.5m
	Gain	54dB
	Scanning mode	Vertically pointing
	Beam width	0.4°
Receiver	Noise	5.8dB
	Noise power	-103dBm
Vertical resolution		30m

For a cloudy profile, the radar CTH is determined as the height of the cloudy bin at the highest level. For cloudy profiles in a period, the radar CTH is the mean CTH of all cloudy profiles. For comparison with satellite data, for multilayer clouds in a period, the CTH is also the average CTH of all cloudy profiles even if the upper-level clouds do not cover the lower-level cloud, rather than the average CTH of the upper-level clouds. For a cloudy profile, the cloud base height (CBH) is determined by the lowest cloudy radar bin. The cloud depth (CD) is equal to the CTH minus the CBH. The final CBH (or CD) is the average value of all CBHs (or CDs).

3. Comparison scheme

A MODIS or AHI CTH data covers larger area than a single profile of radar CTH data. Their data repetition frequency is also different. Thus, temporal and spatial collocation of the radar, MODIS and AHI data is critical to facilitate effective comparison and evaluation.

3.1 Collocation of the Ka radar and MODIS

MODIS CTH data (1 km resolution) measured transiently cover an area of about 1 km2; however, radar takes about 1.7 min to scan a 1 km "line" and about 8 min for a 5 km path if the wind is 10 m s−1. To compensate for the temporal and spatial

differences in the data, Naud and Muller (2002) used MODIS CTH data averaged over a ±0.1 latitude–longitude box for

140   comparison with surface radar data. Dong et al. (2008) used the surface data (on the Southern Great Plains (SGP)

atmospheric observatory established by the Atmospheric Radiation Measurement (ARM)) averaged over a 1 h interval and

the satellite data averaged within a 30 km × 30 km area for the surface–satellite comparison. In Holz et al. (2008), the 5 km

averaged CALIOP data were collocated with the 1 km MODIS data. Chang et al. (2010) used the aircraft lidar CTH data

averaged over a 10 s interval for comparison with satellite measurements. These collocation methods were designed to match

145   the research goal.

At the IAP site, a collocation scheme was determined according to the local conditions. The moving speed and direction

of clouds are always changing and the MODIS spatial resolution has been increased to 1 km, but also varies (Fig. 2).

According to the climatological distribution of clouds, the ground-based CTH measurements from the Ka radar were

averaged within 10 min of the MODIS observation time (±5min) in this study. All the MODIS CTHs within 5 km of the IAP

150   site were extracted and averaged to compare with surface measurements.
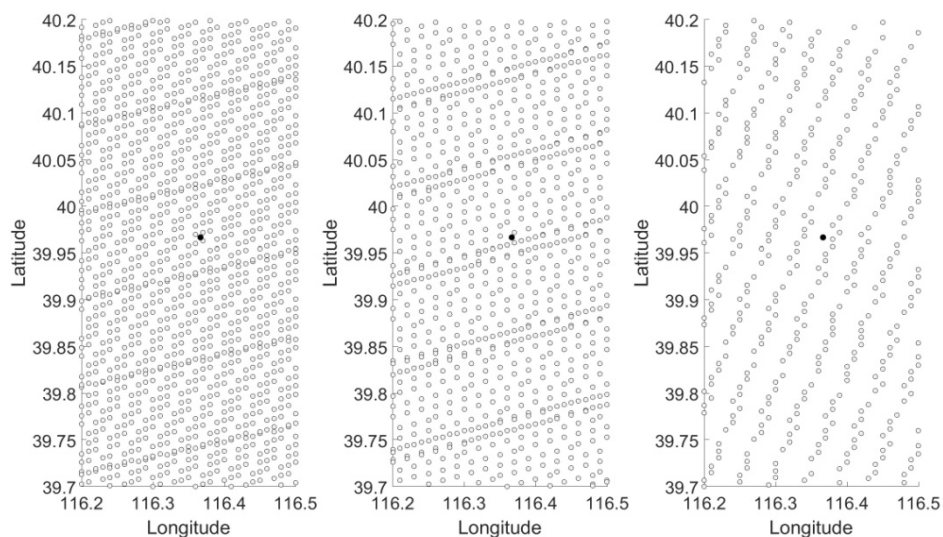
Fig. 2 Locations of the Terra MODIS CTHs (circles) and the Ka-band radar (black solid dots) at the IAP. The three panels show three different spatial resolutions of MODIS CTH datasets around the IAP site because its distance to the sub-satellite point changes as the satellite overpasses.

155

3.2 Ka radar and AHI

AHI CTH data have a fixed 5 km spatial resolution and 10 min temporal resolution over the IAP site (Fig. 3). Since the AHI presents data every 10 min, the measurements of the Ka radar within 10 min of the AHI overpass were extracted and averaged (AHI observation time ±5 min). The AHI CTHs nearest to the IAP site were used for comparison.

160
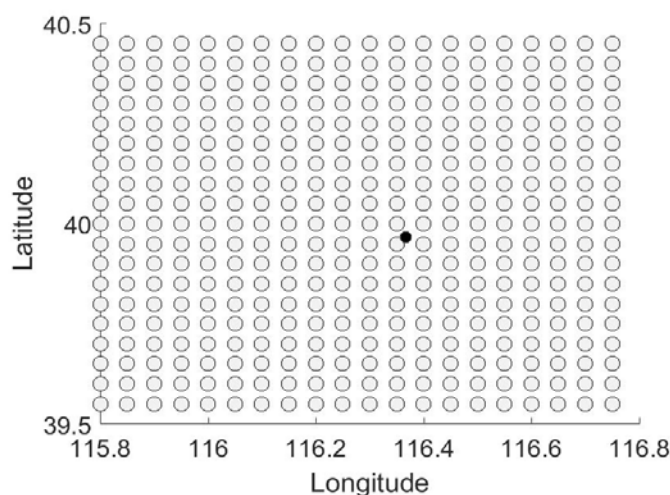
Fig. 3. Locations of the AHI CTHs (circles) and the Ka-band radar (black solid dots) at the IAP. The spatial resolution of the AHI CTH data of full disk is same.

4. Comparison results

In this study, the CTH difference between the radar and MODIS (AHI) data is defined as:

165
$$D_{mr}\ (D_{ar}) = H_m\ (H_a) - H_r \qquad (4)$$

where H_r is the radar CTH, H_m is the MODIS CTH and H_a is the AHI CTH.

This study uses the radar and satellite data observed from 1 January 2016 to 31 December 2017 to evaluate the MODIS and AHI CTHs.

4.1 Comparison between Ka radar and MODIS

170   After discarding clear-sky or poor-quality data, Ka radar and MODIS had 963 valid CTH comparison pairs from 1 January 2016 to 31 December 2017 (Fig. 4). The correlation coefficient between MODIS CTHs and radar CTHs was 0.72, which

showed good agreement with each other. Relative to the Ka radar, MODIS tended to underestimate the CTHs, statistically, by −1.10 ± 2.53 km. Among all comparisons, about 14% differences were less than 0.25 km, 27% were less than 0.5 km and 49% were within 1.0 km.
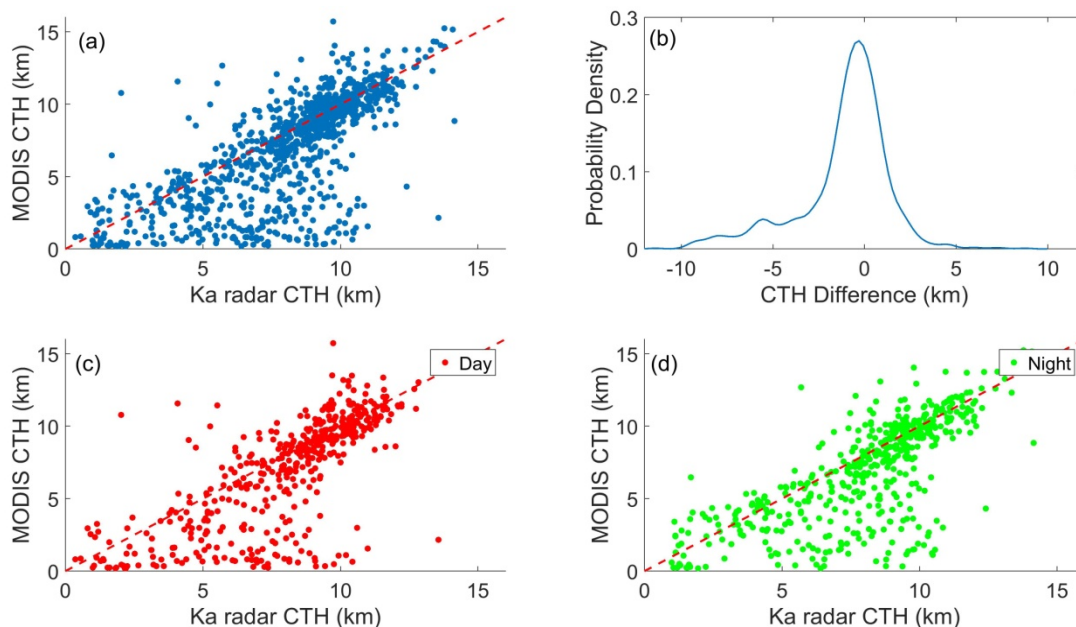
Fig. 4. MODIS CTHs and the Ka-band radar CTHs. (a) All comparisons. (b) The probability density distribution of the D_{mr} (MODIS CTH minus radar CTH). (c) Comparisons at daytime. (d) Comparisons at nighttime.

From Fig. 4a, it can be seen that most of the underestimated data occurred when the retrieved MODIS CTHs were lower

180 than 4 km. Among all comparisons, 62% of MODIS CTHs were greater than 6 km and their average D_{mr} was 0.0026 ± 1.43 km; yet, the average D_{mr} was −3.55 ± 2.99 km when the MODIS CTHs were less than 4 km. Compared with the data with lower MODIS CTH values, MODIS CTHs greater than 6 km showed better agreement with the Ka radar data. That is, if a retrieved MODIS CTH is greater than 6 km, then the probability that the value is close to the true CTH is greater than that for a MODIS CTH less than 4 km. Comparisons between day and night showed that the average D_{mr} values during the day

185 and night were close to each other (Fig. 4c,d). Terra MODIS and Aqua MODIS showed similar accuracy in the CTH retrieval over Beijing.

Uncertainties in the MODIS CTH retrieval depend strongly on cloud depth (Fig. 5). When clouds become thicker, the range of D_{mr} narrows gradually toward zero. Furthermore, the absolute D_{mr} decreases with increasing CD (Table 2). Large differences are mainly due to thin clouds (CD < 1 km). For clouds with CD > 1 km, the average D_{mr} was −0.48 ± 1.70 km,

190   and the average D_{mr} was −0.29 ± 1.43 km for CD > 2 km.
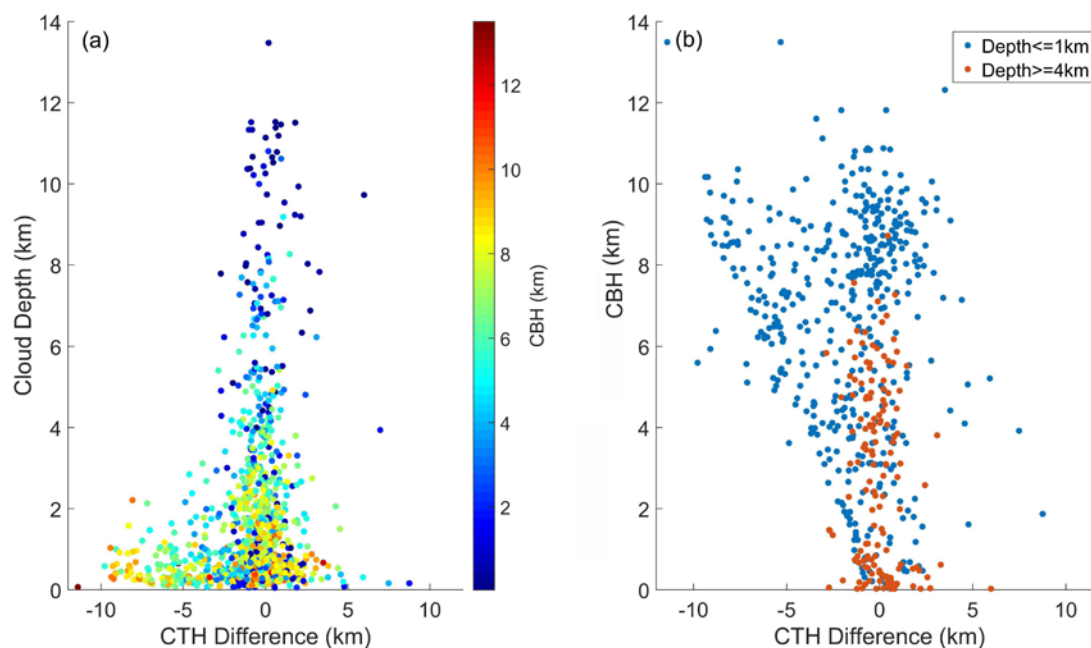
Fig. 5. (a) CTH differences between MODIS and Ka radar decrease as CD increases. (b) Relationship between the CTH difference and the cloud base height (CBH) under two kinds of conditions: cloud depths <=1 km (blue) and >=4 km (orange).

195

Figure 5b shows that the range of D_{mr} changed little as the CBH increased when the CD was greater than 4 km. This means that there is no obvious relationship between D_{mr} and CBH for thick clouds. However, for thin clouds of CD < 1 km, MODIS tended to greatly underestimate the CTH of high-level clouds, especially for the clouds with CBH > 4 km. Clouds with CBH > 4 km and CD < 1 km accounted for 37% of all comparisons, and the average D_{mr} was −2.16 ± 3.17 km. Clouds

200   of CBH < 4 km and CD < 1km account for 10% of all cases, and the average D_{mr} was −0.37 ± 2.07 km. Here, it is found that the MODIS retrieval algorithm shows large uncertainties for thin clouds when the CBH is >4 km and CD is <1 km.

Table 2 Mean and standard deviation of D_{mr} for different CDs (mean ± s.d.) (unit: km)

CD	∈(0,1]	∈(1,2]	∈(2,3]	∈(3,4]	∈(4,5]	>5
D_{mr}	−1.74 ± 3.04	−0.91 ± 2.17	−0.60 ± 1.61	−0.18 ± 1.45	−0.24 ± 1.00	0.01 ± 1.30

Among all 963 comparisons, 753 comparisons had only one cloud layer. For single-layer clouds, the average D_{mr} was

−1.06 ± 2.39 km, while it was −1.23 ± 2.98 km for multilayer clouds. Cloud occurrence frequency (COF) is determined by

the ratio of the cloud time to observation time. We found that the average D_{mr} declined to −0.39 ± 1.57 km for the

comparisons when the CD was >1 km and the COF was >0.5. Here, the MODIS retrieval algorithm showed higher accuracy

for continuous clouds than for broken clouds.

4.2 Comparison between Ka-radar and AHI

Figure 6 shows CTHs from the radar and AHI over 10 h on 9 May 2016. Compared with the MODIS data, the number of

comparison points increased due to the increase in temporal resolution of the data. From 1 January 2016 to 31 December

2017, 6719 valid comparisons were found for the CTH comparison between the radar and AHI.
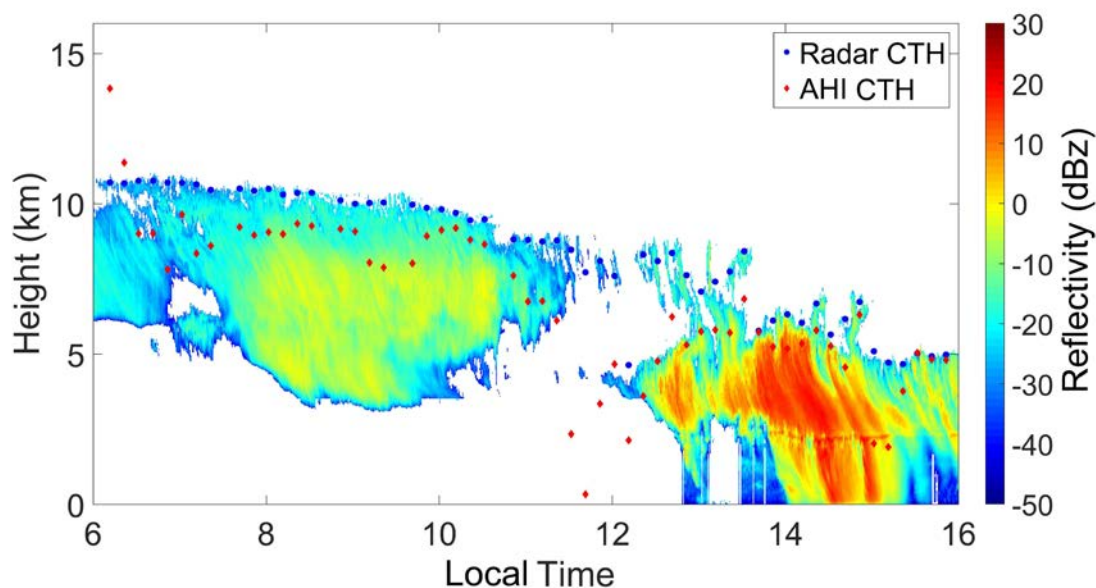
Fig. 6. Ka-radar CTHs (blue filled circles) and the AHI CTHs (red diamonds) on 9 May 2016 from 06:00 to 16:00 (local
time: UTC +8).

It can be seen from Fig. 6 that most AHI CTHs were lower than the radar CTHs. All of the 6719 CTH comparison points

are shown in Fig. 7. Statistically, the average D_{ar} was -1.10 ± 2.27 km. About 11% of the differences were less than 0.25 km,

22% were within and 0.5 km and 42% were within 1.0 km. The average D_{ar} was close to the average D_{mr}, but the standard

220 deviation was lower due to more comparisons. From the statistics based on two years' data, the AHI CTH retrieval algorithm

showed a similar accuracy to the MODIS algorithm when compared with surface radar data.
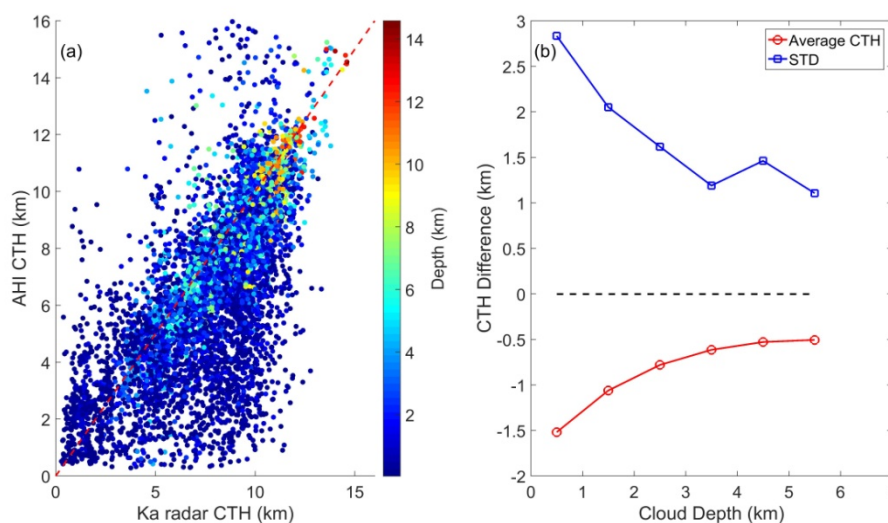
Fig. 7. (a) Ka radar CTHs and the AHI CTHs for all comparison points. (b) The mean CTH difference (AHI CTH − radar CTH) and the standard deviations within different CD ranges.

225

Cloud depth is also a critical factor impacting the accuracy of the AHI retrieval algorithm (Fig. 7b). The average D_{ar}

decreased as the CD increased, i.e., the average D_{ar} was -1.52 ± 2.84 for CD < 1 km while the D_{ar} declined to -0.76 ± 1.63

km for CD > 1 km. The AHI CTHs showed great variations for thin clouds (CD < 1 km). The relationship between the D_{ar}

and the cloud optical thickness (COT) was compared with that between the D_{ar} and CD (Fig. 8). The COTs were from the

230 AHI dataset. The range of the D_{ar} values narrowed as the COT increased, but the distribution was much more scattered than

that for CD, which might due to the COT retrieval errors.
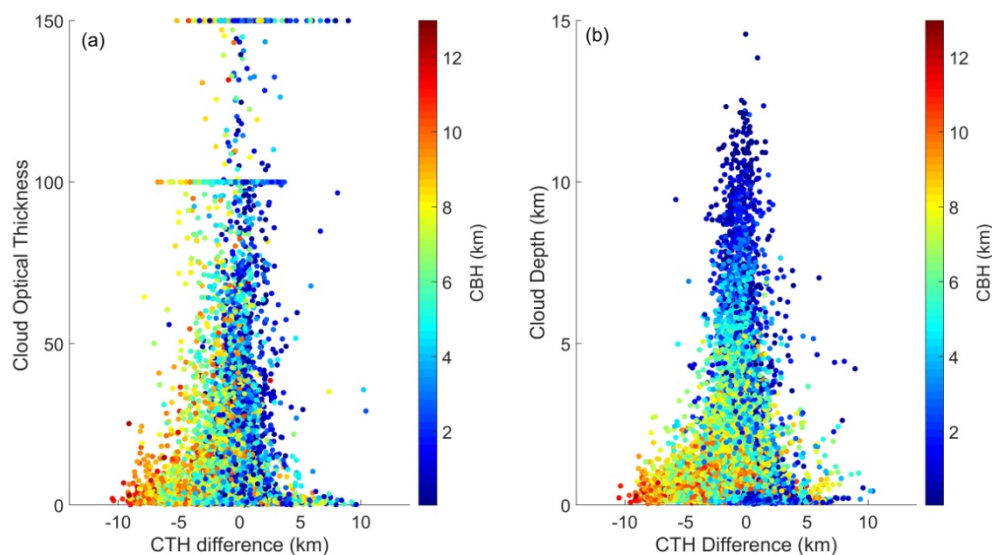
Fig. 8. Relationship between the CTH differences and (a) COT and (b) CD.

235 Among all comparisons, 79% had only one cloud layer. For single-layer clouds, the average D_{ar} was −1.12 ± 2.25 km, while it was −0.99 ± 2.40 km for multilayer clouds. Compared with MODIS, the AHI retrieval algorithm showed a slightly better performance for multilayer clouds. The impact of occurrence frequency on the retrieval accuracy could not be determined because most of the comparisons with CD > 1 km also had occurrence frequencies greater than 0.5.

4.3 Comparison between MODIS and AHI

240 As just addressed, MODIS and AHI CTH data have different spatial and temporal resolutions. This section compares the MODIS CTHs with the AHI CTHs applying two spatial collocation methods: area in 2.5 km radius and in 5 km radius around IAP site. Observation time interval of comparisons is limited within 5 min. More than 600 valid comparisons are matched and are shown in Fig. 9. The mean CTH difference between AHI and MODIS (AHI − MODIS) was −0.70 ± 2.49 km for the 2.5 km collocation and −0.64± 2.36 km for the 5 km collocation. Statistically, the 5 km collocation method

245 showed a smaller difference in the CTHs. The results were similar to Kouki et al. (2016), who reported that the mean AHI

CTH was smaller than the MODIS CTH by −0.54 km based on measurements over 13 days in August. Also, the CTH differences showed an obvious relationship with COT.
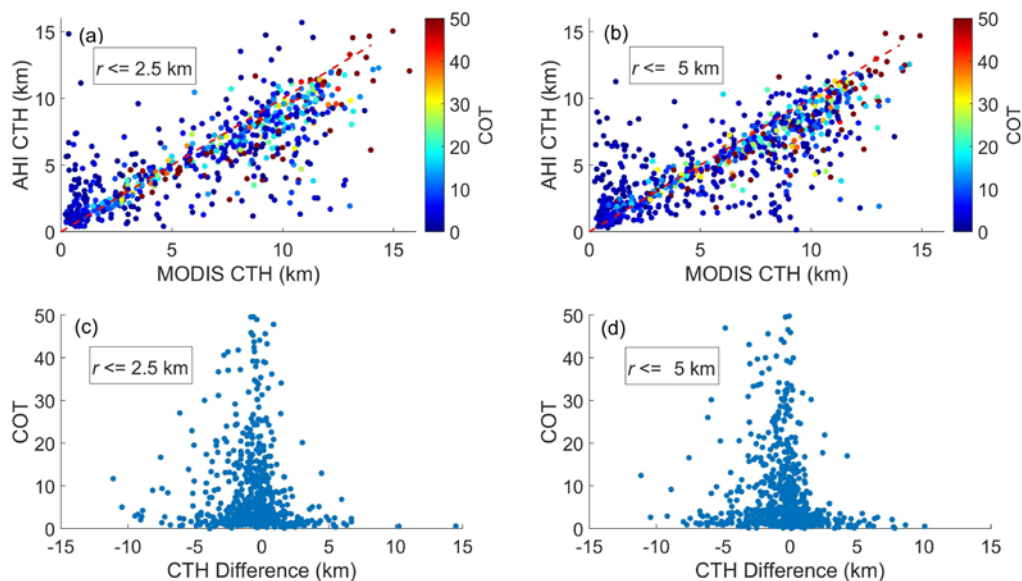
Fig. 9. MODIS CTHs and the AHI CTHs of all comparisons using two collocation areas: (a) area in 2.5 km radius (r) and (b) in 5 km radius. (c), (d) Relationship between the CTH difference and the COT for r ⩽ 2.5 km (c) and r ⩽ 5 km (d).

4.4 Seasonal variation

Beijing is in North China and has a typical continental monsoon climate. It is located in the subtropical monsoon zone, with southwest and southeast monsoons prevailing in summer and the northwest monsoon prevailing in winter. Rainfall is greater in summer, with less rain but more snow occurring in winter. The cloud distribution also shows strong seasonal variations. The monthly averaged D_{mr} and D_{ar} are calculated and presented in Fig. 10 as a reference for the meteorological application of the CTH datasets.
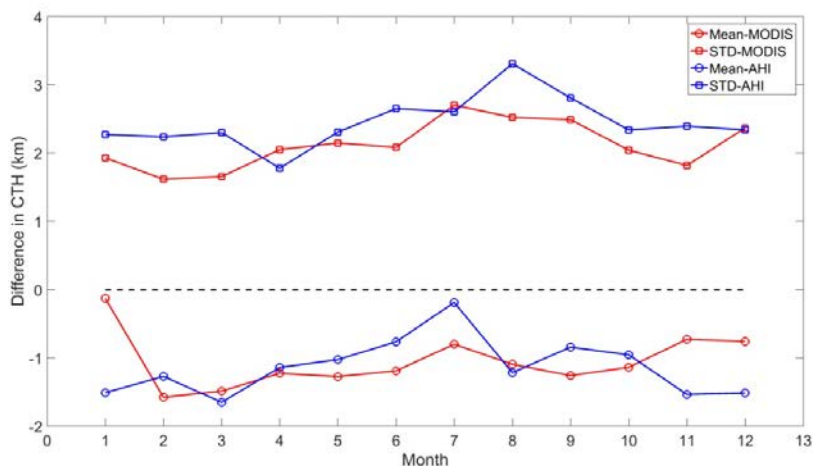
Fig. 10. Monthly variation of the mean CTH differences (circle) and their standard deviations (square) between the radar and
260   the MODIS (red), and the radar and the AHI (blue).

The monthly variation of the D_{ar} was greater than the D_{mr} and showed seasonal characteristics. The AHI retrieval

algorithm had the lowest uncertainty in summer (June–August), while it had the largest uncertainty in winter. As for the

MODIS CTH retrieval algorithm, the lowest accuracy occurred in spring.

265   **5. Summary**

The accuracy of the CTH retrieval algorithm of passive satellite sensors is associated with the instrument, such as the

calibration, signal-noise ratio, the spectral response function and the retrieval algorithm itself, i.e., the atmospheric profile,

the calculation accuracy of the radiative transfer model and uncertainty of the theoretical assumptions. In an effort to better

understand the performance of satellite CTH retrieval algorithms for Beijing, this study evaluated the accuracy of the

270   MODIS and AHI CTH datasets with ground-based radar data based on two years of data.

Overall, the CTHs retrieved from the two passive sensors onboard satellites (Aqua/Terra and HW8) were underestimated

by 1.1 km compared with the surface radar data. Furthermore, the retrieval accuracy strongly depended on cloud depth. As

the retrieval algorithms determine that the CTH retrieved mostly represents the position of the radiation center of the clouds,

it is reasonable that most retrieved CTHs are lower than the radar CTHs.

275   It was found that retrieved MODIS CTHs greater than 6 km were more accurate than those lower than 4 km because they were closer to the radar CTHs. The large differences were mainly from thin clouds (CD < 1 km). In particular, retrieval differences were enlarged when the CBH was greater than 4 km. The average D_{mr} for clouds with CD > 1 km was −0.48 ± 1.70 km, and it was −0.29 ± 1.43 km fore clouds with CD > 2 km. As for the AHI, the average D_{ar} decreased as CD increased, i.e., the average D_{ar} was −1.52 ± 2.84 for CD < 1 km while the D_{ar} declined to −0.76 ± 1.63 km for CD > 1 km.

280   Statistical analysis showed that the average AHI CTHs were lower than the MODIS CTHs by −0.64 ± 2.36 km over Beijing. Statistically, the AHI retrieval algorithm showed better performance for multilayer clouds than single-layer clouds. On the basis of two years of data, the seasonal changes in the CTH retrieval bias for both sensors was also studied. The AHI retrieval algorithm has the lowest bias in summer and the largest bias in winter; the MODIS CTH retrieval algorithm has the lowest accuracy in spring.

285   This study shows the CTH retrieval accuracy of MODIS and AHI, and provides a reference for better understanding the climatological trends of clouds based on satellite datasets and to enhance their application in GCM models. However, this study does not consider the causes of the retrieval uncertainties. By combining the results of this study with an analysis of the raw radiance data and source retrieval codes, more insights into improvement of the retrieval algorithms can be obtained in the future.

290   **Data Availability**

The MODIS product data were obtained from http://ladsweb.nascom.nasa.gov. The AHI data were obtained from https://www.eorc.jaxa.jp/ptree/index.html. The radar data used here are available by special request to the corresponding author (huojuan@mail.iap.ac.cn).

Author contribution

295   Juan Huo and Daren Lu designed the comparisons and Juan Huo carried them out. Shu Duan and Yongheng Bi prepared the

ground-based radar data. Bo Liu prepared some Himawari data and references. Juan Huo prepared the manuscript with

contributions from all co-authors

Competing interests

The authors declare that they have no conflict of interest.

300   **Acknowledgments**

This work is supported by the National Natural Science Foundation of China (grants 41775032 and 41275040). We

appreciate valuable suggestions and insightful instructions from the reviewers. Thanks to the MODIS and the AHI team for

sharing their product datasets. We also acknowledge our Ka-radar team for their maintenance service during long-term

measurements that made our research possible.

305   **References**

Ackerman, S. A., Strabala, K. I., Menzel, W. P., Frey, R. A., Moeller, C. C., and Gumley, L. E.: Discriminating clear sky from
        clouds with MODIS, J. Geophys. Res., 103(D24), 32141-32157, 1998.

Arakawa, A.: The cumulus parameterization problem: Past, present, and future, J. Clim., 17, 2493–2525, 2004.

Atlas, D.: The estimation of cloud parameters by radar, J. Meteor., 11(4), 309-317, 1954.

310   Baum, B. A., Menzel, W. P., Frey, R. A., Tobin, D. C., Holz, R. E., Ackerman, S. A., Heidinger, A. K.,and Yang, P.: MODIS
        cloud-top property refinements for Collection 6, J. Appl. Meteor., 51(6), 1145-1163, 2012.

Bessho, K., Date, K., Hayashi, M., Ikeda, A., Imai, T., Inoue, H., Kumagai, Y., Miyakawa, T., Murata, H., Ohno, T., Okuyama,
        A., Oyama, R., Sasaki, Y., Shimazu, Y., Shimoji, K., Sumida, Y., Suzuki, M., Taniguchi, H., Tsuchiyama, H., Uesawa, D.,
        Yokota, H., and Yoshida, R.:An introduction to Himawari-8/9—Japan's new-generation geostationary meteorological
315   satellites, Journal of the Meteorological Society of Japan, Ser. II, 94(2), 151-183, 2016.

Boucher, O., Randall, D., Artaxo, P., Bretherton, C., Feingold, G., Forster, P., et al.: Clouds and aerosols, in Climate Change 2013: The physical science basis. Contribution of working group I to the fifth assessment report of the Intergovernmental Panel on Climate Change, edited by T. F. Stocker et al.,. Cambridge Univ. Press,Cambridge, U. K., and New York, 2013.

Cess, R. D., Zhang, M. H., Zhou, Y., Jing, X., and Dvortsov, V.: Absorption of solar radiation by clouds: Interpretations of satellite, surface, and aircraft measurements, J. Geophys. Res., 101(D18), 23299-23309, 1996.

Chang, F. L., Minnis, P., Ayers, J. K., McGill, M. J., Palikonda, R., Spangenberg, D. A., Smith Jr., W. L., and Yost, C. R.: Evaluation of satellite‐based upper troposphere cloud top height retrievals in multilayer cloud conditions during TC4, J. Geophys. Res., 115(D10), 2010.

Dong, X., Minnis, P., Xi, B., Sun‐Mack, S., and Chen, Y.: Comparison of CERES‐MODIS stratus cloud properties with ground‐based measurements at the DOE ARM Southern Great Plains site, J. Geophys. Res. Atmos., 113(D3), doi:10.1029/2007JD008438, 2008.

Eyre J. R.: A fast radiative transfer model for satellite sounding systems. ECMWF Research Dept. Tech. Memo. 176, 1991.

Görsdorf, U., Lehmann, V., Bauer-Pfundstein, M., Peters, G., Vavriv, D., Vinogradov, V., and Volkov, V.: A 35-GHz polarimetric Doppler radar for long-term observations of cloud parameters—Description of system and data processing, J. Atmos. Oceanic Technol., 32(4), 675-690, 2015.

Ham, S. H., Sohn, B. J., Yang, P., and Baum, B. A.: Assessment of the quality of MODIS cloud products from radiance simulations, J. Appl. Meteor., 48, 1591-1612, 2009.

Hamada, A., and Nishi, N.: Development of a cloud-top height estimation method by geostationary satellite split-window measurements trained with CloudSat data, J. Appl. Meteor., 49(9), 2035-2049, 2010.

Hamann, U., Walther, A., Baum, B., Bennartz, R., Bugliaro, L., Derrien, M., Francis, P.N., Heidinger, A., Joro, S., Kniffka, A., Gléau, H. L., Lockhoff, M., Lutz, H. J., Meirink, J. F., Minnis, P., Palikonda, R., Roebeling, R., Thoss, A., Platnick, S., Watts, P., Wind, G.: Remote sensing of cloud top pressure/height from SEVIRI: analysis of ten current retrieval algorithms, Atmos. Meas. Tech. Discuss, 7(9), 2839-2867, 2014.

Huo, J., and Lu, D.: Cloud determination of all-sky images under low-visibility conditions, J. Atmos. Oceanic Technol., 26(10), 2172-2181, 2009.

Huo, J., Bi, Y., Lü, D., and Duan, S.: Cloud Classification and Distribution of Cloud Types in Beijing Using Ka-Band Radar Data, Adv. Atmos. Sci., 36(8), 793-803, 2019.

King, M., Tsay, S., Platnick, S.,Wang, M., and Liou, K.: Cloud Retrieval: Algorithms for MODIS: Optical thickness, effective particle radius, and thermodynamic phase. Algorithm Theoretical Basis Document ATBD-MOD-05,83pp.,1998

Kouki, M., Hiroshi, S., Ryo, Y., and Toshiharu, I.: Algorithm theoretical basis document for cloud top height product, Meteorolgical Satellite Center Technical Note, https://www.data.jma.go.jp/mscweb/technotes/msctechrep61-63.pdf, 2016.

Liou, K. N.: Radiation and cloud rrocesses in the atmosphere: theory,observation, and modeling, Oxford University Press, 487 pp, 1992.

Marchand, R.: Trends in ISCCP, MISR, and MODIS cloud-top-height and optical-depth histograms, J. Geophys. Res., , 118, 1941-1949, 2013.

Marchand, R., Ackerman, T., Smyth, M., and Rossow, W. B.: A review of cloud top height and optical depth histograms from MISR, ISCCP, and MODIS, J. Geophys. Res., 115, http://dx.doi.org/10.1029/2009JD013422, 2010.

Min, M., Wu, C., Li, C., Liu, H., Xu, N., Wu, X., Chen, L., Wang, F., Sun, F., Qin, D., Wang, X., Li, B., Zheng, Z., Cao, G. and Dong, L.: Developing the science product algorithm testbed for Chinese next-generation geostationary meteorological satellites: FengYun-4 series, J. Meteor. Res., 31(4), 708-719, 2017.

Mouri, K., Izumi, T., Suzue, H., and Yoshida, R.: Algorithm Theoritical Basis Document of cloud type/phase product. Meteorological Satellite Center Technical Note, 61, 19-31.

Naud, C., Muller, J. P., and Clothiaux, E. E.: Comparison of cloud top heights derived from MISR stereo and MODIS CO_2 ‐ slicing, Geophys. Res. Lett., 29(16), 42-1, 2002.

Nieman, S. J., Schmetz, J., and Menzel, W. P.: A comparison of several techniques to assign heights to cloud tracers, J. Appl. Meteorol., 32(9), 1559-1568, 1993.

Pavolonis, M. J., and Heidinger, A. K.: Daytime cloud overlap detection from AVHRR and VIIRS, J. Appl. Meteorol., 43(5), 762-778, 2004.

Pincus, R., Platnick, S., Ackerman, S. A., Hemler, R. S., and Patrick Hofmann, R. J.: Reconciling simulated and observed views of clouds: MODIS, ISCCP, and the limits of instrument simulators, J. Clim., 25(13), 4699-4720, 2012.

Remer, L. A., Kleidman, R. G., Levy, R. C., Kaufman, Y. J., Tanré, D., Mattoo, S., Martins, J. V., Ichoku, C., Koren, I., Yu, H. and Holben, B. N.: Global aerosol climatology from the MODIS satellite sensors, J. Geophys. Res., 113(D14), DOI:10.1029/2007JD009661, 2008.

Ramanathan, V. L. R. D., Cess, R. D., Harrison, E. F., Minnis, P., Barkstrom, B. R., Ahmad, E., and Hartmann, D.: Cloud-radiative forcing and climate: Results from the Earth Radiation Budget Experiment, Science, 243(4887), 57-63, 1989.

Rodell, M., and Houser, P. R.: Updating a land surface model with MODIS-derived snow cover, J. Hydrometeorol., 5(6), 1064-1075, 2004.

Roskovensky, J. K., and Liou, K. N.: Simultaneous determination of aerosol and thin cirrus optical depths over oceans from MODIS data: Some case studies, J. Atmos. Sci., 63(9), 2307-2323, 2006.

Rossow, W. B., and Schiffer, R. A.: Advances in understanding clouds from ISCCP, Bull. Amer. Meteor. Soc., 80(11), 2261-2288,1999.

Schmetz, J., Holmlund, K., Hoffman, J., and Strauss, B.: Operational cloud motion winds from Meteosat infrared images. J. Appl. Meteorol., 32,1207-1225, 1993.

Schiffer, R. A., and Rossow, W. B.: The International Satellite Cloud Climatology Project (ISCCP): The first project of the
380   world climate research programme, Bull. Am. Meteorol.Soc., 64(7), 779-784, 1983.

Smith, W. L., and Platt, C. M. R.: Comparison of satellite-deduced cloud heights with indications from radiosonde and
       ground-based laser measurements, J. Appl. Meteorol., 17(12), 1796-1802, 1978.

Stephens, G. L., and Kummerow, C. D.: The remote sensing of clouds and precipitation from space: A review, J. Atmosph.
       Sciences, 64(11), 3742-3765, 2007.

385   Stubenrauch, C. J., Del Genio, A. D., and Rossow, W. B.: Implementation of subgrid cloud vertical structure inside a GCM and
       its effect on the radiation budget, J. Clim., 10(2), 273-287, 1997.

Weisz, E., Li, J., Menzel, W. P., Heidinger, A. K., Kahn, B. H., and Liu, C. Y.: Comparison of AIRS, MODIS, CloudSat and
       CALIPSO cloud top height retrievals, Geophys. Res. Lett., 34(17), 2007.

Wetherald, R. T., and Manabe, S.: Cloud feedback processes in a general circulation model, J. Atmos. Sci., 45(8), 1397-1416,
390   1988.

Xi, B., Dong, X., Minnis, P., and Sun‐Mack, S.: Comparison of marine boundary layer cloud properties from CERES‐
       MODIS Edition 4 and DOE ARM AMF measurements at the Azores, J. Geophys. Res. Atmos., 119(15), 9509-9529,
       doi:10.1002/2014JD021813, 2014.

Xiao, P., Huo, J. and Bi, Y., 2018: Ground-based Ka- band cloud radar data quality control. Journal of Chengdu University of
395   Information   Technology.   Journal   of   Chengdu   University   of   Information   Technology,   33,   129-136,
       https://doi.org/110.16836/j.cnki.jcuit.12018.16802.16005.

Zhou, Q., Zhang, Y., Li, B., Li, L., Feng, J., Jia, S., Lv, S., Tao, F. and Guo, J.: Cloud-base and cloud-top heights determined
       from   a   ground-based   cloud   radar   in   Beijing,   China,   Atmosph.   Environm.,   201,   381-390,
       https://doi.org/310.1016/j.atmosenv.2019.1001.1012, 2019.

400